An Assessment of the Ability of the Obstruction-Scaling Model to Estimate Solute Diffusion Coefficients in Hydrogels.

ARTICLE *in* JOURNAL OF CONTROLLED RELEASE · DECEMBER 2014

Impact Factor: 7.71 · DOI: 10.1016/j.jconrel.2014.12.010 · Source: PubMed

2 AUTHORS, INCLUDING:

Brian Amsden
Queen's University
120 PUBLICATIONS **3,472** CITATIONS

SEE PROFILE

Journal of Controlled Release 199 (2015) 10–16

Contents lists available at ScienceDirect

Journal of Controlled Release

journal homepage: www.elsevier.com/locate/jconrel

An assessment of the ability of the obstruction-scaling model to estimate solute diffusion coefficients in hydrogels

Nicholas A. Hadjiev, Brian G. Amsden *

Department of Chemical Engineering, Queen's University, Kingston, ON K7L 3N6, Canada

ARTICLE INFO

Article history:
Received 9 October 2014
Revised 4 December 2014
Accepted 6 December 2014
Available online 10 December 2014

Keywords:
FRAP
Diffusion in hydrogels
Mathematical model
Diffusion in polymer solutions

ABSTRACT

The ability to estimate the diffusion coefficient of a solute within hydrogels has important application in the design and analysis of hydrogels used in drug delivery, tissue engineering, and regenerative medicine. A number of mathematical models have been derived for this purpose; however, they often rely on fitted parameters and so have limited predictive capability. Herein we assess the ability of the obstruction-scaling model to provide reasonable estimates of solute diffusion coefficients within hydrogels, as well as the assumption that a hydrogel can be represented as an entangled polymer solution of an equivalent concentration. Fluorescein isothiocyanate dextran solutes were loaded into sodium alginate solutions as well as hydrogels of different polymer volume fractions formed from photoinitiated cross-linking of methacrylate sodium alginate. The tracer diffusion coefficients of these solutes were measured using fluorescence recovery after photobleaching (FRAP). The measured diffusion coefficients were then compared to the values predicted by the obstruction-scaling model. The model predictions were within ±15% of the measured values, suggesting that the model can provide useful estimates of solute diffusion coefficients within hydrogels and solutions. Moreover, solutes diffusing in both sodium alginate solutions and hydrogels were demonstrated to experience the same degree of solute mobility restriction given the same effective polymer concentration, supporting the assumption that a hydrogel can be represented as an entangled polymer solution of equivalent concentration.

1. Introduction

Solute diffusion within a hydrogel is an important phenomenon in a number of research fields, including pharmaceutics and regenerative medicine. For the rational design of controlled release devices [1,2], as well as for the assessment of drug distribution within tissue or intracellularly following release or upon administration [3–5] and for the survival and function of encapsulated cells implanted as artificial organs [6,7] or for regenerative purposes [8,9], it would be highly useful to have a mathematical expression that provides reliable estimates of solute diffusion coefficients within hydrogels and that relies solely on physical property measurements of the solute and the polymer. A number of mathematical expressions have been derived for this purpose [10,11], yet no model is capable of providing a priori predictions of the solute diffusion coefficient without relying on fitted parameters. A mathematical expression based on obstructive effects has been shown to predict the influence of solute size as well as polymer properties, such as chain flexibility, degree of ionization, and chain radius, on the solute diffusion coefficient within both nonionic and charged hydrogels [12–14]. Thus, it was posited that the model could be adapted to provide a priori predictions for solute diffusion coefficients within hydrogels.

The model is based on the premise that solute diffusion is controlled by the ability of the solute to find a series of openings between the polymer chains large enough to allow its passage, a mechanism initially proposed by Yasuda et al. [15]. The diffusion coefficient of the solute within the swollen hydrogel, D, is given by,

$$D = D_o \exp\left[-\pi\left(\frac{R + r_f}{\xi + 2r_f}\right)^2\right] \quad (1)$$

in which D_o is the diffusion coefficient in the aqueous medium in the absence of the polymer, R is the radius of the solute probe, r_f is the polymer chain radius, and ξ is the correlation length, which represents the average mesh size of the network [16].

The development of Eq. (1) was based on a number of assumptions, including: 1) the solute is a hard sphere, 2) there are negligible intermolecular forces of attraction between the solute and the polymer chains, 3) the polymer chains act only as physical obstacles in the diffusive process, 4) the polymer chains are immobile relative to the mobility of the solute over the time scale of the diffusion process, and 5) the distribution of openings between polymer chains can be approximated by a random distribution of straight fibers, described by the Ogston expression [17]. These assumptions restrict the applicability of the model to situations that satisfy these conditions. By the first assumption, the model is not applicable to situations where the solute can reptate. The

* Corresponding author.
E-mail address: amsden@queensu.ca (B.G. Amsden).

http://dx.doi.org/10.1016/j.jconrel.2014.12.010
0168-3659/

second assumption requires that any potential interaction forces between the solute and the polymer are weak. That the polymer chains are immobile with respect to the movement of the solute molecule has been previously validated for solute diffusion in polymer solutions by considering the relative time scales for solute translation versus polymer chain segment movement over an equivalent distance [18]. Finally, in order to derive the model, a means of calculating the average mesh size necessitated the adoption of an idealized geometry of the polymer chains within the network. The Ogston expression for the distribution of spherical spaces between a random arrangement of straight chains was used as a first approximation, despite the fact that the polymer chains in hydrogels are semi-flexible. The use of this expression yielded very good agreement between the obstruction-scaling model and available data [12], suggesting its potential for representing the spherical spaces between semi-flexible polymer chains. Furthermore, it has been demonstrated recently through simulations of solute partitioning into hydrogels composed of chains of varying chain stiffness, that the Ogston model of the distribution of spherical spaces between polymer chains is applicable to cross-linked polymer networks composed of flexible, semi-flexible, and stiff chains [19].

To use Eq. (1) requires values for the solute radius, the polymer chain radius, and the correlation length. In this study nonionic fluorescein isothiocyanate labeled dextrans were used to ensure that there were negligible forces of interaction between the diffusing solute and the alginate. Dextran is a random coil in solution, and so the appropriate radius to use to assess its restricted mobility within a polymer hydrogel or aqueous solution is its radius of gyration. The chain radius can be calculated from the polymer specific volume by assuming that each monomer can be approximated as a cylinder (vide infra). What remains is a means of calculating the correlation length of the network.

It is assumed that the correlation length of a hydrogel is the same as that of a solution of uncrosslinked linear chains of the same polymer at an equivalent concentration. For polymer solutions, the scaling relationship proposed by De Gennes for concentrations greater than the overlap concentration can be used to estimate the correlation length [16] as,

$$\xi = R_g\left(c^*/c\right)^{\nu}. \tag{2}$$

In Eq. (2), c is the polymer solution concentration, c* is the concentration at which the polymer chains begin to overlap in solution, R_g is the radius of gyration of the polymer, and ν is a scaling coefficient, which has a theoretical value of 0.75 for a good solvent, 1 for a theta solvent, and 0.5 for a marginal solvent [20,21]. Combining Eqs. (1) and (2) yields,

$$D = D_o \exp\left[-\pi\left(\frac{R + r_f}{R_g\left(c^*/c\right)^{\nu} + 2r_f}\right)^2\right]. \tag{3}$$

The polymer solution overlap concentration can be calculated from [22],

$$c^* = \frac{3M}{4\pi N_A R_g^3} \tag{4}$$

in which M is the weight average molecular weight of the polymer, and N_A is Avogadro's constant [16].

Polymer concentration within hydrogels is usually expressed in terms of volume fraction, ϕ, in which case Eq. (2) becomes,

$$\xi = R_g\left(\phi^*/\phi\right)^{\nu}. \tag{5}$$

The solute diffusion coefficient within the hydrogel expression then becomes,

$$D = D_o \exp\left[-\pi\left(\frac{R + r_f}{R_g\left(\phi^*/\phi\right)^{\nu} + 2r_f}\right)^2\right] \tag{6}$$

in which $\phi^* = \nu c^*$ and ν is the specific volume of the polymer.

The objective of this study was to assess the ability of Eq. (6) to provide accurate predictions of the diffusion coefficient of a solute in a hydrogel. In the process, the validity of the assumption that the correlation length of a polymer solution is the same as that of the same polymer in a gel state at an equivalent concentration would also be determined. Sodium alginate was used to prepare hydrogels for this study. Sodium alginate was chosen for a number of reasons. It is widely investigated as a drug delivery and cell bioencapsulation material [23], its physical properties are well characterized, it can be used as an analog for solute diffusion within the extracellular matrix due to its compositional similarity to many extracellular matrix polysaccharides that are also negatively charged [24], and it was used previously for testing the model against diffusion in polymer solutions [18], thereby providing a means of direct comparisons. Alginate hydrogels are typically formed through the ionotropic interaction between the guluronate monomer blocks with divalent cations such as calcium [25]. However, hydrogels formed in this fashion would deviate significantly from the assumed hydrogel structure of an entangled polymer solution. To form hydrogels with only short covalent cross-link points between polymer chains, the sodium alginate was methacrylated and then cross-linked using photoinitated free radical polymerization. The tracer diffusion coefficients of fluorescently labeled dextrans (4, 10, 20 kDa) within alginate hydrogels of varying alginate volume fraction were measured using fluorescence recovery after photobleaching (FRAP) and then compared against the values predicted by Eq. (6).

2. Materials and methods

Unless otherwise stated, all materials were used as received.

2.1. Sodium alginate methacrylation

Methacrylated alginate (MALG) was prepared by reacting sodium alginate with 2-aminoethyl methacrylate, as described by Jeon et al. [26] Sodium alginate, isolated from *Laminaria hyperborea* stipe (Protanal LF 10/60) was obtained from FMC Biopolymer, Drammen, Norway. To prepare MALG, 4.0 g sodium alginate was dissolved in 0.2 L deionized water (Millipore Milli-Q Plus, 18 mΩ cm) over the course of a few hours with periodic stirring by vortex. The resulting solution was diluted with a morpholine buffer to prepare a 0.4 L mixture comprised of 1% sodium alginate (w/v), 0.5 M NaCl (Fisher Scientific), and 50 mM 2-morpholinoethanesulfonic acid (MES, Fisher) at pH 6.5. To activate the carboxyl moieties on the native alginate, 1.06 g N-hydroxysuccinimide (NHS, Acros Organics) and 3.50 g N-(3-dimethylaminopropyl)-N′-ethylcarbodiimide hydrochloride (EDC, Acros Organics) were dissolved in the sodium alginate solution; the activation reaction was conducted under constant agitation for 5 min at pH 6.5. After 5 min, 1.52 g 2-aminoethyl methacrylate hydrochloride (AEMA, Polysciences) and 50 ppm hydroquinone monomethyl ether (MEHQ, Sigma Aldrich) were added and the reaction was maintained at the preceding activation conditions for an additional 24 h in the absence of light. The product (0.4 L) was admixed with a phosphate buffer to prepare a 0.6 L solution of 0.5 M sodium dihydrogen phosphate (Sigma Aldrich) that was left stirring for 24 h at pH 5.0 in the absence of light. The resulting mixture was purified by dialysis (MWCO: 3500, Fisherbrand) against 4.0 L deionized water for 4 days (medium replaced at 2, 4, 8, 24, 48, 72, and 96 h), vacuum filtered (Whatman 42, Nalgene

0.2 μm RapidFlow Thermo Scientific), frozen, and lyophilized. The degree of methacrylation was determined from ^{1}H NMR spectra obtained on a Bruker Avance-400 spectrometer equipped with a BBFO probe. The spectra were obtained at 80 °C with the MALG was dissolved at 30 mg/mL in deuterium oxide. The degree of methacrylation was calculated from the ratio of the integration of the peaks corresponding to the vinyl protons on the methacrylate group ($\delta = 6.2$ and 6.7 ppm) to those of the C5 and C1 protons on the alginate guluronate monomers ($\delta = 5$ and 5.2, and 5.6 ppm, respectively) and the C1 proton on the mannuronate monomers ($\delta = 5.2$ ppm) [27].

2.2. Preparation of hydrogels via photopolymerization

The hydrogels were formed via UV-initiated free radical polymerization using 2-hydroxy-1-[4-(2-hydroxyethoxy) phenyl]-2-methyl-1-propanone (I2959, Sigma Aldrich, Canada) as a photoinitiator. To prepare hydrogels used for FRAP measurements, MALG was dissolved in a morpholine buffer comprised of 0.01 M MES, 0.22 M NaCl, and 4.5 mM I2959 at pH 7.2 over the course of a few hours while stirring. The resulting solution was centrifuged at 3000 rpm for 2 min (Centra CL2 Thermo Scientific IEC), poured into a mold (Lab-Tek Chamber Slide, 16 well × 0.15 cm^3), and photopolymerized using UV light (365 nm) at 35 mW/cm^2 for 4 min (Hamamatsu LC8 Lightning Cure). The hydrogels were soaked in a 4.0 L buffer solution of 0.01 M MES, 0.22 M NaCl, and 0.01% sodium azide at pH 7.2 for 72 h to extract the sol content. The volume fraction of alginate in the hydrogels, and thus the cross-link density of the hydrogels, was varied by adjusting the concentration of the MALG in each sample. The polymer volume fraction within the hydrogels was determined using a mass balance and the following equation,

$$\phi = \frac{m_g \rho_p}{m_p \rho_g} \tag{7}$$

in which m_p is the mass of dry alginate in the gel, m_g is the mass of the hydrated hydrogel, ρ_p is the alginate density (1.66 g/cm^3) [17], and ρ_g is the density of the hydrogel, taken to be 1 g/cm^3. To obtain the mass values, the hydrogels were weighed when wet, then frozen, lyophilized, and weighed when dry. To determine the efficiency of the cross-linking process, MALG was dissolved in type I purified water to which I2959 was added at the concentration noted above, poured into the molds and photo-cross-linked using the conditions described above. Immediately following photo-cross-linking, the gels were frozen in liquid nitrogen. The frozen hydrogels were lyophilized and their dry mass recorded. The dried samples were then swollen in type I purified water at room temperature, with the water replaced three times every 2 h. The hydrogels were again frozen in liquid nitrogen and lyophilized and the final mass measured. The sol content was calculated as the difference in dried mass before and after extraction divided by the mass of dried sample before extraction.

2.3. Determination of tracer diffusion coefficients

The hydrogels were loaded with fluorescein isothiocyanate labeled dextran of varying molecular weight (4, 10, and 20 kDa (Sigma Aldrich), referred to hereafter as FDX4, FDX10, and FDX20, respectively) by soaking them in a buffer solution of 0.01 M MES, 0.22 M NaCl, 0.01% sodium azide, and 1 mg/mL FDX at pH 7.2 for two days in the absence of light. The concentration of the FDX was within the limits of the concentration range in which a linear relationship exists between the final fluorescence signal and the concentration of the agent, as verified in the study by Braeckmans et al. [28]. Polymer solutions were prepared by dissolving sodium alginate or MALG (5, 10, 15, and 20 mg/mL) in the MES buffer containing 1 mg/mL FDX. These solutions were stored for two days alongside the hydrogels in the absence of light during their loading to ensure consistency in the methods. The tracer diffusion coefficients of fluorescein isothiocyanate labeled bovine serum albumin (FITC–BSA) in solutions of sodium alginate were measured to validate the FRAP measurement protocol. For these experiments, 4.0 mg/mL FITC–BSA solutions were prepared in a buffer of 0.01 M MES, 0.22 M NaCl, 0.01% sodium azide, at pH 7.2 containing sodium alginate concentrations of 5, 10, 15, and 20 mg/mL. Prior to using FITC–BSA, the linear concentration profile of its fluorescence versus concentration was confirmed by measuring the intensity of its fluorescence in buffer solutions at concentrations ranging from 1–4 mg/mL. The concentration for the FITC–BSA was selected to be 4.0 mg/mL, to compensate for the faint signal of this probe.

The FRAP experiments were performed at ambient temperature on an Olympus FluoView-1000 confocal scanning laser microscope using a 10× objective lens (UPLSAP010x, NA 0.4) in the absence of a simultaneous scanner. A 488 nm multi-line argon laser (30 mW) was used for excitation of the FITC-labeled fluorophores and their emitted fluorescence was detected using a 510–550 nm band pass filter. Photoannihilation of the sample was carried out by using a combination of the 488 and 405 nm lasers (50 mW, 80 mW total) set to full intensity. A custom imaging slide was prepared by using a polystyrene petri dish (Fisherbrand 60 × 15 mm) that was modified with a 0.17 mm (standard #1.5) glass cover slip (Fig. 1). The dish was first perforated by heating a steel cylindrical punch that was used to bore the plastic bottom. The puncture was then sanded and leveled to a smooth surface prior to applying the cover slip. The glass cover slip was fixed on to the bottom of the petri dish with a combination of high vacuum grease (Dow Corning) and quick set glue (Super Glue).

All FRAP measurements were conducted using the FV-10 ASW ver. 3.0 software package provided by Olympus. The sample was first secured on to the stage of the CSLM and brought into focus at a depth that extended 100 μm from the surface of the glass cover slip. The FITC dye was then selected from the chromophore database and the confocal aperture opened to 80 μm or 1 airy unit for optimal sectioning. The intensity of the 488 nm laser line was initially set to 10% and then subsequently decreased in succession with a gradual increase in the high voltage to balance low power illumination with fluorescence detection. The high voltage was limited to 700 V to avoid introducing additional noise. Using this approach, the laser line was generally configured to 2% of its full power, thereby providing a strong fluorescence signal and adequate attenuation to minimize the effects of bleaching when recording. The gain was set to 1.0 for all FRAP measurements. The offset was set at 0 to ensure consistency between samples. FRAP measurements were carried out after drawing a region of interest (ROI) disk of specific diameter in the bleaching software using a tornado scan. The diameter of these disks was determined by a simple calibration protocol that fit the size of the ROI to a known free diffusion coefficient for a specific fluorochrome. The image acquisition settings were set to capture 800 frames total (200 pre-bleach and 600 post-bleach) with the photoannihilation sequence fixed at 110 ms for all measurements, unless specified otherwise. The zoom factor and image resolution were set to 7 times and 320 × 320 pixels, respectively, while the user-defined field of view was cropped by 80–90% to increase the frame rate, resulting in up to ~10 frames/s using a unidirectional scan.

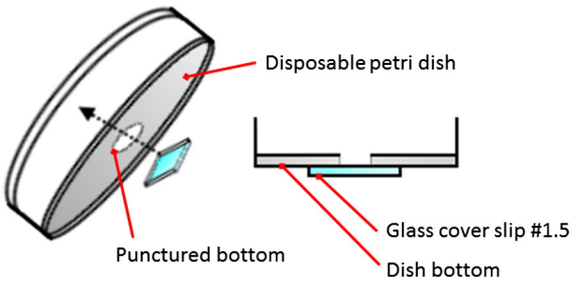

Fig. 1. Customized imaging slide used in the FRAP measurements.

To calibrate the ROI, the solute of interest (either FDX or FITC–BSA) was dissolved in deionized water at a concentration below the upper limit of its linear profile, filtered through a syringe filter (0.22 μm, Fisherbrand), and injected into the well of the customized imaging slide. The well was covered with a glass cover slip that was coated with a thin layer of vacuum grease to generate a strong seal between the slip and the petri dish to minimize the effects of convection. The sample was secured to the stage of the CSLM and allowed to reach equilibrium. The diameter of the ROI was then calibrated to the value of the diffusion coefficient of the specific solute at infinite dilution, D_o, prior to proceeding with image acquisition or photobleaching. FRAP data were obtained using the FV-10 ASW ver. 3.0 software package provided by Olympus. The data extraction was carried out by collecting the fluorescence intensity for each image within a stack over the time frame of a single FRAP experiment for the photobleaching disk and its reference region, which was an exact copy of the ROI in a location that was not affected by the photoannihilation sequence. The distance between the two regions was sufficiently large to avoid influence from either signal. The diffusion coefficient was calculated via a non-linear least squares fitting algorithm in Graphpad Prism 6 to the data using the uniform disk model (UDM) derived by Braeckmans et al. [28].

2.4. FDX molecular weight

The weight average molecular weight of the FDX solutes was measured using gel permeation chromatography with combined refractive index and right angle laser light scattering detectors. The polymers were dissolved in 0.05 M $NaNO_3$, 0.02% w/v sodium azide in deionized water and the solutions injected into a Malvern Viscotek GPCmax VE 2001 equipped with a TDA triple detector array and utilizing PolyAnalytik PAA-202.5, 203, and 204 columns with a flow rate of 1.0 mL/min.

3. Results and discussion

The protocol used for preparing the hydrogels was based on the methodology reported by Jeon et al. [26]. That a hydrogel was effectively formed in our hands by the photo-cross-linking method was confirmed by measuring the sol content of the resulting networks. The sol content in every case was less than 0.04, indicating successful network formation. The cross-link density of the hydrogels was varied by manipulating the concentration of MALG used to prepare the hydrogels. The equilibrium swollen polymer volume fractions of the hydrogels ranged from 0.0025 to 0.0293.

3.1. Determination of FDX properties

The diffusion coefficients of the solutes at infinite dilute (D_o) were needed to determine the ROI for the FRAP measurements. These values were calculated using the Stokes–Einstein equation at the recorded temperature of the experiment and using the hydrodynamic radius of the solute. The hydrodynamic radius of BSA was taken to be 3.5 nm [18]. For the FDX solutes, data from Doucet et al. [29], Wallace et al. [30], and de Smedt et al. [31] for FDX of varying molecular weight were curve fit (Fig. 2) to generate the following equation relating hydrodynamic radius, R_h, to FDX weight average molecular weight, M_w,

$$R_h = 0.0163\, M_w^{0.52}. \quad (8)$$

Eq. (8) was then used along with the weight average molecular weights of the FDX obtained measured using GPC to calculate the D_o values given in Table 1.

The radius of gyration of each FDX solute (R_{gFDX}) was obtained from a curve fit of the data of Andrieux et al. [32] of the radii of gyration of FDX of varying weight average molecular weights and narrow dispersity (Fig. 3), resulting in the following equation,

$$R_{gFDX} = 0.022(M_w)^{0.5}. \quad (9)$$

Eq. (9) was then used to calculate R_g for each FDX solute using the measured weight average molecular weight. These values are also listed in Table 1.

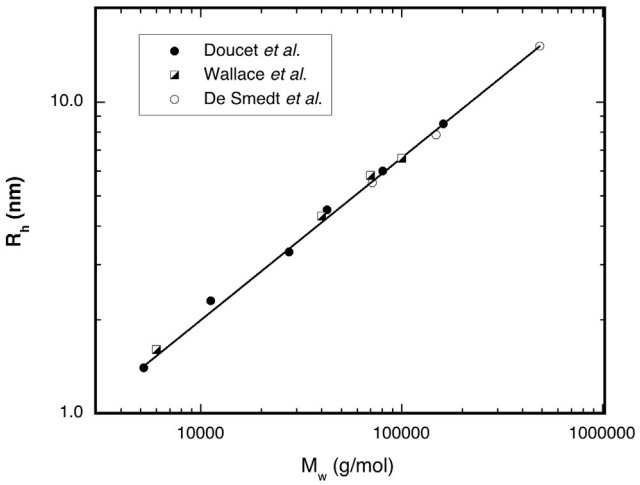

Fig. 2. Relationship between FITC-dextran hydrodynamic radius, R_h, and weight average molecular weight, M_w. The data were taken from Doucet et al. [29], Wallace et al. [30], and de Smedt et al. [31]. The solid line represents a curve fit to the data.

3.2. Validation of the FRAP protocol

To validate the FRAP methodology used, the tracer diffusion coefficients of FITC–BSA in LF10/60 sodium alginate solutions of varying concentrations were measured and compared to those reported by Zhang and Amsden measured using pulsed field gradient NMR (PFG-NMR) [18]. The results are given in Fig. 4 as the ratio of the diffusion coefficient measured of BSA in the polymer solution (D) to that of BSA diffusing in water at infinite dilution (D_o). The very close agreement between the values obtained using the two different techniques was taken as validation of the FRAP methodology used.

The tracer diffusion coefficients of the FDX solute probes in the MALG hydrogels of varying sodium alginate volume fraction were then measured by FRAP and compared to the predictions of the obstruction model. To apply the model required values of the solvent scaling parameter, v, the radius of the sodium alginate polymer chain and its radius of gyration. The scaling parameter for sodium alginate in aqueous solution was determined by Wang et al. to be 0.5 using small-angle X-ray scattering [33]. At 13% methacrylation, the physical properties of the MALG were assumed to be comparable to the unmodified sodium alginate and the scaling parameter was, therefore, selected to be 0.5. The cross-sectional bare chain radius of sodium alginate has also been determined by Wang et al. to be 0.55 nm [33]. This value was adjusted to include a water layer upon polymer hydration by adding the diameter of a water molecule (0.28 nm) to the measured radius. The resulting chain radius of the unmodified, hydrated sodium alginate (r_f) is thereby

Table 1
Physical properties of the FITC-dextran (FDX) probes used in the FRAP experiments.

Solute	M_w (kg/mol)	R_h (nm)	D_o ($\times 10^7$ cm^2/s)	R_{gFDX} (nm)
FDX4	4.8	1.3	16.3	1.5
FDX10	10.7	2.0	10.9	2.2
FDX20	20.1	2.8	7.8	3.1

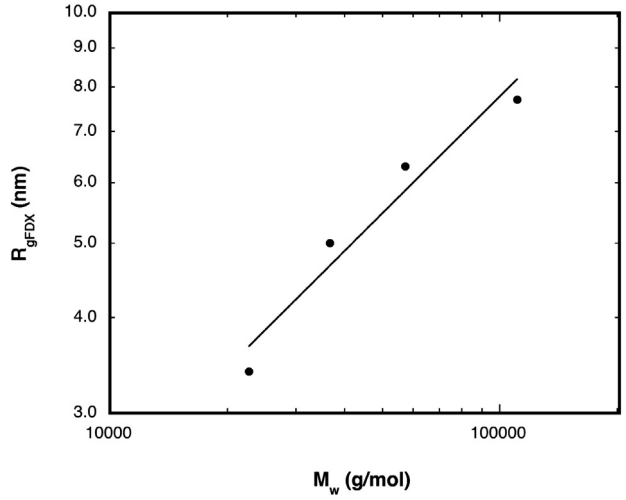

Fig. 3. Relationship between FITC-dextran radius of gyration, R_{gFDX}, and weight average molecular weight, M_w. The data were taken from Andrieux et al. [32]. The solid line represents a curve fit to the data.

0.83 nm. The polymer chain radius of the MALG was estimated using a mole-weighted average of the radius of alginate residues and the radius of methacrylated alginate residues by applying the following expression,

$$r_f = \left(\frac{M_m \upsilon}{\ell \pi N_A}\right)^{\frac{1}{2}} \tag{10}$$

in which M_m is the molecular weight of the monomer, ℓ is the specific length of the monomer, and ν is the specific volume of the polymer. The average radius for the MALG was estimated to be 0.84 nm, which is only slightly different than unmodified sodium alginate. Moreover, once cross-linked, the oligomethacrylate blocks formed would not significantly contribute to the obstructive effect of the chain radius. As a result, the cross-sectional polymer chain for the hydrogels was selected to be 0.83 nm.

Donati et al. [34] measured the radius of gyration of LF 10/60 sodium alginate (R_{gALG}) to be 56.9 nm and its weight average molecular weight to be 126 kDa using high-performance size-exclusion chromatography coupled with multi-angle laser light scattering (HPSEC-RI-MALLS). In the study of Donati et al., the eluent for the HPSEC-RI-MALLS was 0.05 M Na_2SO_4 and 0.01 M ethylenediaminetetraacetic acid (EDTA) at pH 6.0. Excluding minor contributions by the EDTA and sodium alginate, the ionic strength of the eluent used in the experiment by Donati et al. was 0.15 M. The buffer used in all FRAP experiments had an ionic strength of approximately 0.22 M. The majority of the electrostatic interactions between the polymer chains are effectively screened at 0.15 M [18], and so the radius of gyration of the sodium alginate should not change at 0.22 M or pH 7.2. This assumption is supported by the finding that the radius of gyration of alginate with a guluronic acid mol fraction of 38% remained constant above an ionic strength of 0.1 M [35]. The ^{1}H NMR analysis indicated that the degree of methacrylation of the sodium alginate was 13%. Again, recognizing that the oligomethacrylate blocks would not contribute significantly to the influence of the polymer chains on solute mobility within the network, the radius of gyration of sodium alginate was therefore taken to be 56.9 nm for the application of the model to the diffusion data.

3.3. Assessment of the obstruction-scaling model

The ratio of the measured tracer diffusion coefficient of each FDX solute in a MALG hydrogel to its respective calculated D_o value is shown in Fig. 5 as a function of the alginate volume fraction of the hydrogel. Also in Fig. 5 are the model predictions, shown as the curves. The model predictions are in good agreement with the data; for each data set, the model prediction yielded coefficients of determination (R^2) greater than 0.87 (Table 2).

To test the assumption that the correlation length of a hydrogel is equivalent to that of a solution of that polymer having the same polymer volume fraction, tracer diffusion coefficients were also measured for FDX10 and FDX20 in sodium alginate (ALG) solutions of varying polymer volume fraction. These results are plotted as D / D_o and compared to the D / D_o values of these solutes measured in MALG gels, and with the model predictions, in Fig. 6.

The D / D_o values lie along the same curve, regardless of whether the solute was diffusing in a polymer solution or a hydrogel. This result suggests that polymer solutions and cross-linked networks at equivalent polymer volume fractions provide the same degree of solute mobility restriction, supporting the assumption that the correlation length of a polymer gel can be considered equivalent to that of a polymer solution of the same concentration. This finding is reasonable given that the polymer chains have been shown to be essentially immobile in comparison to the solute mobility in a polymer solution [18], and the introduction of covalent crosslinks would only reduce polymer chain motion in a

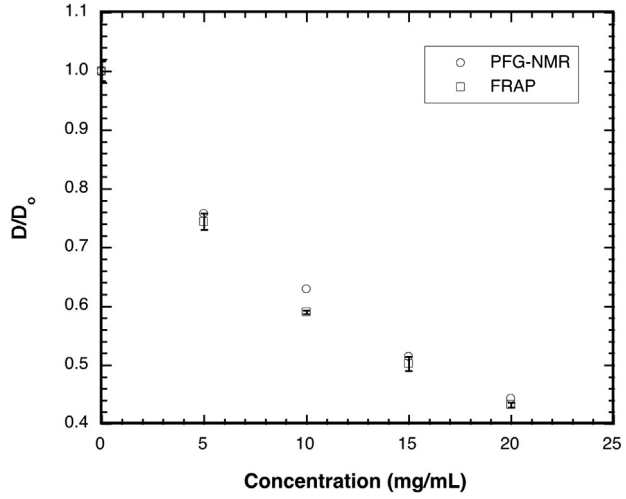

Fig. 4. Comparison of measurements of BSA tracer diffusion coefficients in LF10/60 sodium alginate solutions made using the FRAP protocol versus those made by Zhang and Amsden using pulsed field gradient NMR (PFG-NMR) [18]. For the FRAP results, each data point is an average of three measurements and the error bars represent the standard deviation.

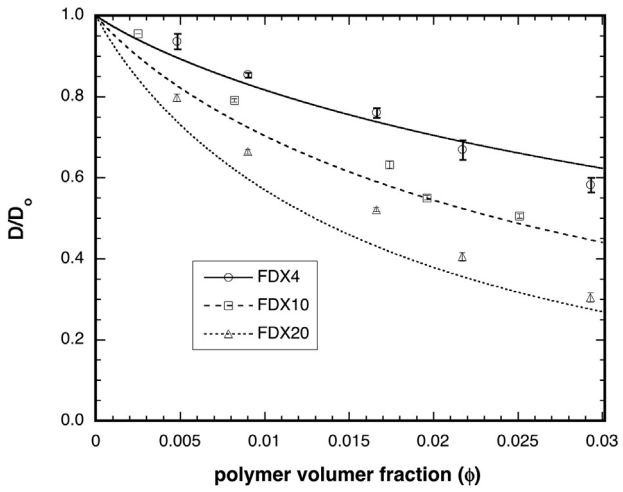

Fig. 5. Comparison of model predictions to FRAP data of FDX tracer diffusion coefficients within the MALG hydrogels. The curves represent the trend predicted by Eq. (6). Each data point is an average of three measurements and the error bars represent the standard deviation.

Table 2
Coefficient of determination (R^2) values of the model predictions for the different FDX solutes.

Solute	R^2
FDX4	0.935
FDX10	0.937
FDX20	0.876

hydrogel. The finding also suggests that if the data were plotted as D / D_o versus $(R_{gFDX} + r_f) / (\xi + 2r_f)$ the data would collapse to a single curve. As shown in Fig. 7, the experimental data does collapse around the predicted curve. It is notable that all the data but for one data point falls within the 15% relative error envelope indicated by the dashed curves in Fig. 7.

The model can thus be considered to provide very good a priori estimates (to within approximately ± 15% of the measured value) of the D / D_o value of a solute probe within a polymer solution or cross-linked network, employing measurable polymer and solute properties, provided the assumptions underlying its derivation are valid for the situation under consideration. Nevertheless, the model has been tested against a relatively small data set, as there is a lack of reports of solute diffusion in hydrogels wherein all the physical parameters required to assess the model predictions have been measured. The model needs to be applied to a broader range of hydrogel systems to confirm its predictive capabilities.

With respect to formulation development, drug diffusion is the most broadly applicable release mechanism from hydrogels. Having a tool that can be used to provide accurate estimates of the diffusion coefficient would allow for rapid screening of potential polymer compositions and their influence on solute diffusion from hydrogels made from these polymers. The dominant parameter in determining the diffusion coefficient within the gels is the radius of gyration of the prepolymer. Further, R_g is a measure of polymer chain flexibility, architecture, and solvent–polymer interactions, and mathematical expressions for the influence of each of these effects are available in the literature [36]. Knowing how R_g changes with these parameters can then be used to predict their effect on drug release from a device made from these polymers. The model could also be used as a basis for developing further mathematical expressions that incorporate polymer–drug interactions. Finally, the model can be used for estimating the distribution of a drug following release from any device into the surrounding biological environments, which are often well represented as hydrogels.

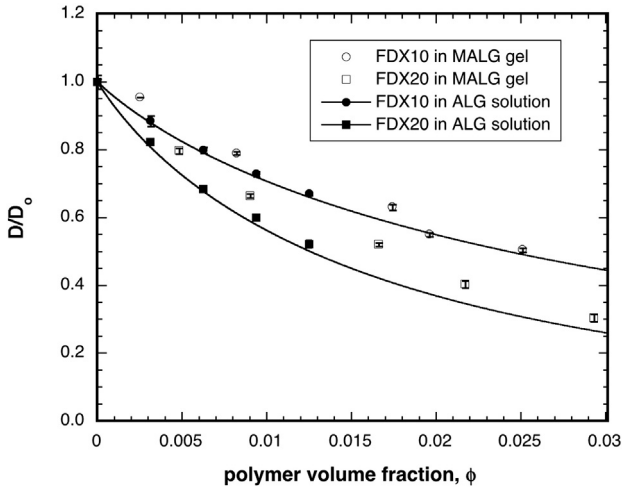

Fig. 6. Comparison of reduced FDX tracer diffusion coefficients within MALG hydrogels to those within sodium alginate (ALG) solutions. The curves represent the trend predicted by Eq. (6). Each data point is an average of three measurements and the error bars represent the standard deviation.

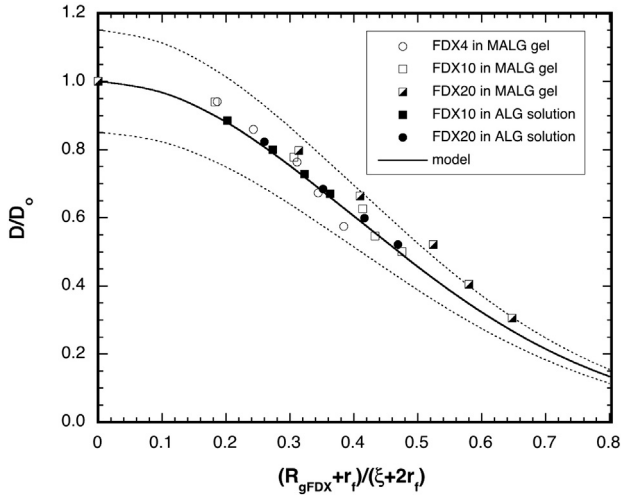

Fig. 7. Comparison of solute diffusion within hydrogels and polymer solutions plotted as the dimensionless parameters D / D_o vs. $(R_{gFDX} + r_f) / (\xi + 2r_f)$. The model predictions are indicated as the solid line, while the dashed lines represent a relative error envelope of ± 15% around the model prediction.

4. Conclusions

To assess the predictive capability of a previously derived mathematical model based on obstruction effects to describe solute diffusion in a hydrogel, FRAP measurements of the tracer diffusion of fluorescein isothiocyanate conjugated dextrans of varying molecular weight were obtained in hydrogels prepared from methacrylated sodium alginate and in solutions of sodium alginate. Very good agreement was obtained between the FRAP data and the model predictions. Moreover, solute mobility was demonstrated to be restricted to the same degree for a hydrogel of an equivalent concentration as a polymer solution, supporting the assumption that the correlation length of a hydrogel is equivalent to that of a solution of its prepolymer at the same concentration. These findings suggest that the model is capable of providing reasonable a priori predictions of the diffusion coefficient of a solute within both hydrogels and polymer solutions. It should be noted that the model has been applied only to hydrogels at swelling equilibrium, and in many situations involving hydrogel delivery systems, the hydrogel is subject to swelling following exposure to physiological fluids. In these situations, the hydrogel properties are changing with time, and therefore, so is the solute diffusion coefficient. Nonetheless, the model provided in this paper could provide a means of predicting the temporal change in solute diffusion coefficient as the gel system swells if expressions for changes in the polymer volume fraction of the hydrogel with time could be determined.

Acknowledgments

The authors gratefully acknowledge operational funding from the Natural Sciences and Engineering Research Council of Canada through the 20/20 Ophthalmic Biomaterials, and infrastructure support from the Canadian Foundation for Innovation and the Ontario Research Infrastructure Fund.

References

[1] T. Vermonden, S.S. Jena, D. Barriet, R. Censi, J. van der Gucht, W.E. Hennink, et al., Macromolecular diffusion in self-assembling biodegradable thermosensitive hydrogels, Macromolecules 43 (2010) 782–789, http://dx.doi.org/10.1021/ma902186e.
[2] C.-C. Lin, A.T. Metters, Hydrogels in controlled release formulations: network design and mathematical modeling, Adv. Drug Deliv. Rev. 58 (2006) 1379–1408, http://dx.doi.org/10.1016/j.addr.2006.09.004.
[3] Q. Xu, N.J. Boylan, J.S. Suk, Y.-Y. Wang, E.A. Nance, J.-C. Yang, et al., Nanoparticle diffusion in, and microrheology of, the bovine vitreous ex vivo, J. Control. Release 167 (2013) 76–84, http://dx.doi.org/10.1016/j.jconrel.2013.01.018.

[4] Y. Cu, W.M. Saltzman, Mathematical modeling of molecular diffusion through mucus, Adv. Drug Deliv. Rev. 61 (2009) 101–114, http://dx.doi.org/10.1016/j.addr.2008.09.006.
[5] E.A. Nance, G.F. Woodworth, K.A. Sailor, T.-Y. Shih, Q. Xu, G. Swaminathan, et al., A dense poly(ethylene glycol) coating improves penetration of large polymeric nanoparticles within brain tissue, Sci. Transl. Med. 4 (2012) 149ra119, http://dx.doi.org/10.1126/scitranslmed.3003594.
[6] J. Kang, G. Erdodi, J.P. Kennedy, H. Chou, L. Lu, S. Grundfest Broniatowski, Toward a bioartificial pancreas: diffusion of insulin and IgG across immunoprotective membranes with controlled hydrophilic channel diameters, Macromol. Biosci. 10 (2010) 369–377, http://dx.doi.org/10.1002/mabi.200900386.
[7] G. Orive, E. Santos, J.L. Pedraz, R.M. Hernández, Application of cell encapsulation for controlled delivery of biological therapeutics, Adv. Drug Deliv. Rev. 67–68 (2014) 3–14, http://dx.doi.org/10.1016/j.addr.2013.07.009.
[8] M. Parlato, W. Murphy, Soluble molecule transport within synthetic hydrogels in comparison to the native extracellular matrix, in: C.J. Connon, I.W. Hamley (Eds.), Hydrogels in Cell-based Therapies, Royal Society of Chemistry, Cambridge, 2014, pp. 1–30, http://dx.doi.org/10.1039/9781782622055-00001.
[9] J.L. Drury, D.J. Mooney, Hydrogels for tissue engineering: scaffold design variables and applications, Biomaterials 24 (2003) 4337–4351, http://dx.doi.org/10.1016/S0142-9612(03)00340-5.
[10] B. Amsden, Solute diffusion within hydrogels. Mechanisms and models, Macromolecules 31 (1998) 8382–8395.
[11] L. Masaro, X.X. Zhu, Physical models of diffusion for polymer solutions, gels and solids, Prog. Polym. Sci. 24 (1999) 731–775, http://dx.doi.org/10.1016/S0079-6700(99)00016-7.
[12] B. Amsden, An obstruction-scaling model for diffusion in homogeneous hydrogels, Macromolecules 32 (1999) 874–879, http://dx.doi.org/10.1021/ma980922a.
[13] B. Amsden, Diffusion in polyelectrolyte hydrogels: application of an obstruction-scaling model to solute diffusion in calcium alginate, Macromolecules 34 (2001) 1430–1435.
[14] B. Amsden, K. Grotheer, D. Angl, Influence of polymer ionization degree on solute diffusion in polyelectrolyte gels, Macromolecules 8 (2002) 3179–3183.
[15] H. Yasuda, L. Ikenberry, C. Lamaze, Permeability of solutes through hydrated polymer membranes. Part II. Permeability of water soluble organic solutes, Makromol. Chem. 125 (1969) 108–118.
[16] P.-G. de Gennes, Scaling Concepts in Polymer Physics, Cornell University Press, 1979.
[17] A. Ogston, The spaces in a uniform suspension of fibres, Trans. Faraday Soc. 54 (1958) 1754–1757.
[18] Y. Zhang, B.G. Amsden, Application of an obstruction-scaling model to diffusion of vitamin B12 and proteins in semidilute alginate solutions, Macromolecules (2006) 1073–1078, http://dx.doi.org/10.1021/ma0522357.
[19] M. Quesada-Pérez, I. Adroher-Benítez, J.A. Maroto-Centeno, Size-exclusion partitioning of neutral solutes in crosslinked polymer networks: a Monte Carlo simulation study, J. Chem. Phys. 140 (2014) 204910, http://dx.doi.org/10.1063/1.4879215.
[20] D. Schaefer, J. Joanny, P. Pincus, Dynamics of semiflexible polymers in solution, Macromolecules 13 (1980) 1280–1289.
[21] D. Schaefer, A unified model for the structure of polymers in semidilute solution, Polymer 25 (1984) 387–394.
[22] I. Teraoka, Polymer Solutions, John Wiley & Sons, 2002.
[23] K.Y. Lee, D.J. Mooney, Alginate: properties and biomedical applications, Prog. Polym. Sci. 37 (2012) 106–126, http://dx.doi.org/10.1016/j.progpolymsci.2011.06.003.
[24] A.D. Augst, H.J. Kong, D.J. Mooney, Alginate hydrogels as biomaterials, Macromol. Biosci. 6 (2006) 623–633, http://dx.doi.org/10.1002/mabi.200600069.
[25] K. Clare, Algin, in: J. BeMiller, R. Whistler (Eds.),Industrial Gums: Polysaccharides and Their Derivatives, Third ed., 1993, pp. 105–143 (Industrial Gums: Polysaccharides and Their Derivatives, London).
[26] O. Jeon, K.H. Bouhadir, J.M. Mansour, E. Alsberg, Photocrosslinked alginate hydrogels with tunable biodegradation rates and mechanical properties, Biomaterials 30 (2009) 2724–2734, http://dx.doi.org/10.1016/j.biomaterials.2009.01.034 (ion protein in a human breast cancer cells expressing EGFR/VEGFR).
[27] T.A. Fenoradosoa, G. Ali, C. Delattre, C. Laroche, E. Petit, A. Wadouachi, et al., Extraction and characterization of an alginate from the brown seaweed *Sargassum turbinarioides* Grunow, J. Appl. Phycol. 22 (2010) 131–137, http://dx.doi.org/10.1007/s10811-009-9432-y.
[28] K. Braeckmans, L. Peeters, N.N. Sanders, S.C. De Smedt, J. Demeester, Three-dimensional fluorescence recovery after photobleaching with the confocal scanning laser microscope, Biophys. J. 85 (2003) 2240–2252, http://dx.doi.org/10.1016/S0006-3495(03)74649-9.
[29] G.J. Doucet, D. Dorman, R. Cueto, D. Neau, P.S. Russo, D. De Kee, et al., Matrix fluorescence photobleaching recovery for polymer molecular weight distributions and other applications, Macromolecules 39 (2006) 9446–9455, http://dx.doi.org/10.1021/ma0608525.
[30] M. Wallace, D.J. Adams, J.A. Iggo, Analysis of the mesh size in a supramolecular hydrogel by PFG-NMR spectroscopy, Soft Matter 9 (2013) 5483–5491, http://dx.doi.org/10.1039/C3SM27793C.
[31] S. de Smedt, A. Lauwers, J. Demeester, Y. Engleborghs, G. de Mey, M. Du, Structural information on hyaluronic acid solutions as studied by probe diffusion experiments, Macromolecules 27 (1994) 141–146.
[32] K. Andrieux, P. Lesieur, S. Lesieur, M. Ollivon, Characterization of fluorescein isothiocyanate-dextrans used in vesicle permeability studies, Anal. Chem. (2002), http://dx.doi.org/10.1021/ac020119l.
[33] Z.Y. Wang, J.W. White, M. Konno, S. Saito, T. Nozawa, A small-angle X-ray scattering study of alginate solution and its Sol–Gel transition by addition of divalent cations, Biopolymers 35 (1995) 227–238, http://dx.doi.org/10.1002/bip.360350211.
[34] I. Donati, A. Coslovi, A. Gamini, G. Skjåk-Braek, A. Vetere, C. Campa, et al., Galactose-substituted alginate 2: conformational aspects, Biomacromolecules 5 (2004) 186–196, http://dx.doi.org/10.1021/bm030063k.
[35] F. Avaltroni, M. Seijo, S. Ulrich, S. Stoll, K.J. Wilkinson, Conformational changes and aggregation of alginic acid as determined by fluorescence correlation spectroscopy, Biomacromolecules 8 (2007) 106–112, http://dx.doi.org/10.1021/bm060655d.
[36] J. Bicerano, Prediction of Polymer Properties, Third edition Marcel Dekker, Inc., New York, 2002.